Published in final edited form as:
J Immunol. 2003 November 15; 171(10): 5188–5197.

T Cell Activation-Induced Mitochondrial Hyperpolarization Is Mediated by Ca^{2+}- and Redox-Dependent Production of Nitric Oxide[1]

Gyorgy Nagy[*], **Agnes Koncz**[*], and **Andras Perl**[2,*,†]

[*]Department of Medicine, State University of New York, College of Medicine, Syracuse, NY 13210

[†]Department of Microbiology and Immunology, State University of New York, College of Medicine, Syracuse, NY 13210

Abstract

Activation, proliferation, or programmed cell death of T lymphocytes is regulated by the mitochondrial transmembrane potential ($\Delta\psi_m$) through controlling ATP synthesis, production of reactive oxygen intermediates (ROI), and release of cell death-inducing factors. Elevation of $\Delta\psi_m$ or mitochondrial hyperpolarization is an early and reversible event associated with both T cell activation and apoptosis. In the present study, T cell activation signals leading to mitochondrial hyperpolarization were investigated. CD3/CD28 costimulation of human PBL elevated cytoplasmic and mitochondrial Ca^{2+} levels, ROI production, and NO production, and elicited mitochondrial hyperpolarization. Although T cell activation-induced Ca^{2+} release, ROI levels, and NO production were diminished by inositol 1,4,5-triphosphate receptor antagonist 2-aminoethoxydiphenyl borane, superoxide dismutase mimic manganese (III) tetrakis (4-benzoic acid) porphyrin chloride, spin trap 5-diisopropoxyphosphoryl-5-methyl-1-pyrroline-*N*-oxide, and NO chelator carboxy-2-phenyl-4,4,5,5-`oxide, mitochondrial hyperpolarization was selectively inhibited by carboxy-2-phenyl-4,4,5,5-tetramethyl-imidazoline-1-oxyl-3-oxide (−85.0 ± 10.0%; $p = 0.008$) and, to a lesser extent, by 2-aminoethoxydiphenyl borane. Moreover, NO precursor (*Z*)-1-[2-(2-aminoethyl)-*N*-(2-ammonioethyl)amino]diazen-1-ium-1,2-diolate diethylenetriamine elicited NO and ROI production, Ca^{2+} release, transient ATP depletion, and robust mitochondrial hyperpolarization (3.5 ± 0.8-fold; $p = 0.002$). Western blot analysis revealed expression of Ca-dependent endothelial NO synthase and neuronal NO synthase isoforms and absence of Ca-independent inducible NO synthase in PBL. CD3/CD28 costimulation or H_2O_2 elicited severalfold elevations of endothelial NO synthase and neuronal NO synthase expression, as compared with β-actin. H_2O_2 also led to moderate mitochondrial hyperpolarization; however, Ca^{2+} influx by ionomycin or Ca^{2+} release from intracellular stores by thapsigargin alone failed to induce NO synthase expression, NO production, or $\Delta\psi_m$ elevation. The results suggest that T cell activation-induced mitochondrial hyperpolarization is mediated by ROI- and Ca^{2+}-dependent NO production.

[1]This work was supported in part by Grants DK 49221 and AI 48079 from the National Institutes of Health and the Central New York Community Foundation.

[2]Address correspondence and reprint requests to Dr. Andras Perl, Department of Medicine, State University of New York, 750 East Adams Street, Syracuse, NY 13210. perla@upstate.edu.

The signaling networks that mediate activation, proliferation, or programmed cell death of T lymphocytes are dependent on complex redox and metabolic pathways. T lymphocytes are primarily activated through the TCR following interaction with a specific peptide/major histocompatibility Ag complex on the APC. The outcome of TCR engagement depends on concomitant signaling through costimulatory molecules (CD28, CD40 ligand, LFA-1, and CD2) and cytokines (1). The Ag-binding αβ- or γδTCR is associated with a multimeric receptor module comprised of the CD3 γδε- and TCR ζ-chains. The cytoplasmic domains of CD3 and ζ-chains contain a common motif, YXX(L/I)$X_{6–8}$ YXX(L/I), termed IgR family tyrosine-based activation motif (ITAM)[3], which is crucial for coupling of intracellular tyrosine kinases (2). Binding of p56^{lck} to CD4 or CD8 attracts this kinase to the TCR ζ/CD3 complex, leading to phosphorylation of ITAM. Phosphorylation of both tyrosines of each ITAM is required for Src homology 2 domain-mediated binding by ζ-associated protein-70 (ZAP-70) or the related SYK. ZAP-70 is activated through phosphorylation by p56^{lck}. Activated ZAP-70 and SYK target two key adaptor proteins, linker for activation of T cells (LAT) and Src homology 2 domain-containing leukocyte protein of 76 kDa (2). Oxidative stress causes diminished phosphorylation and displacement of LAT from the cell membrane of T cells (3). Phosphorylated LAT binds directly to phospholipase C-γ1. Further downstream, phospholipase C-γ1 controls hydrolysis of phosphatydilinositol–4,5-biphosphate to inositol–1,4,5-triphosphate (IP_3) and diacylglycerol. Phosphorylation of inositol lipid second messengers is mediated by phosphatidylinositol 3-hydroxyl kinase (PI_3K). The stimulatory effect of the TCR alone on PI_3K activity is small. Concurrent triggering of the CD28 costimulatory molecule by its ligands CD80 or CD86 is required for optimal PI_3K activation. IP_3 binds to its receptors in the endoplasmic reticulum, opening Ca^{2+} channels that release Ca^{2+} to the cytosol. Sustained increase of intracellular Ca^{2+} levels mediates coupling of ATP production to metabolic need during T cell activation (4). The mitochondrion, the site of oxidative phosphorylation, has long been identified as a source of energy and cell survival. The synthesis of ATP is driven by an electrochemical gradient across the inner mitochondrial membrane maintained by an electron transport chain and the membrane potential (negative inside and positive outside). A small fraction of electrons react directly with oxygen and form reactive oxygen intermediates (ROI). Although ROI have long been considered as toxic by-products of aerobic existence, evidence is now accumulating that controlled levels of ROI modulate various aspects of cellular function and are necessary for signal transduction pathways, including those mediating apoptosis (5).

Mitochondrial ROI production modulates T cell activation, cytokine production, and proliferation at multiple levels (6, 7). Intracellular ROI levels are subject to regulation by an

[3]Abbreviations used in this paper ITAM, IgR family tyrosine-based activation motif; ZAP-70, ζ-associated protein-70; LAT, linker for activation of T cells; IP_3, inositol-1,4,5-triphosphate; PI_3K, phosphatidylinositol 3-hydroxyl kinase; ROI, reactive oxygen intermediate; $\Delta\psi_m$, mitochondrial transmembrane potential; NOS, NO synthase; nNOS, neuronal NOS; eNOS, endothelial NOS; iNOS, inducible NOS; 2-APB, 2-aminoethoxydiphenyl borane; MnTBAP manganese (III) tetrakis (4-benzoic acid) porphyrin chloride DIPPMPO,5-diisopropoxyphosphoryl-5-methyl-1-pyrroline-*N*-oxide C-PTIO, carboxy-2-phenyl-4,4,5,5-tetramethyl-imidazoline-1-oxyl-3-oxide PI, propidium iodide HE, hydroethidine DHR, dihydrorhodamine 123 DCF,5,6-carboxy-2′,7′-dichlorofluorescein $DiOC_6$, 3,3′-dihexyloxacarbocyanine iodide TMRM, tetramethylrhodamine methyl ester DAF-FM,4-amino-5-methylamino-2′,7′-difluoroflourescein diacetate Fluo-3/AM,fluoro-3 acetoxymethyl ester JC-1 5,5′,6,6′-tetrachloro-1,1 ′,3,3′-tetraethylbenzimidazolocarbocyanine iodide NAO, nonyl acridine orange NOC-18,(*Z*)-1-[2-(2-aminoethyl)-*N*-(2-ammonioethyl)amino]diazen-1-ium-1,2-diolate diethylenetriamine SNP, sodium nitroprusside.

oxidation-reduction equilibrium of mitochondrial ROI production and generation of reducing equivalents, pyridine nucleotides (NADH/NAD plus NADPH/NADP) and reduced glutathione levels (8). Elevation of the mitochondrial transmembrane potential ($\Delta\psi_m$) or mitochondrial hyperpolarization has been recently identified as an early event associated with Fas- (9), H_2O_2-(10), HIV-1- (11), p53- (12), TNF-α- (13), and staurosporin-induced apoptosis (14). Mitochondrial hyperpolarization precedes disruption of $\Delta\psi_m$ and activation of caspases, points of no return, during Fas-dependent apoptosis (9). Following exposure to NO, persistent mitochondrial hyperpolarization was recently observed in astrocytes (15). Elevation of $\Delta\psi_m$ is also triggered by activation of the CD3/CD28 complex (5, 16) or stimulation by Con A (9). Therefore, elevation of $\Delta\psi_m$ or mitochondrial hyperpolarization represent an early but reversible switch not exclusively associated with apoptosis. With $\Delta\psi_m$ hyperpolarization and extrusion of H^+ ions from the mitochondrial matrix, the cytochromes within the electron transport chain become more reduced, which favors generation of ROI (17). Thus, mitochondrial hyperpolarization is a likely cause of ROI production at early stages of T cell activation and apoptosis and, thus, represent a key checkpoint in cell fate decision (8).

In the present study, we investigated the ordering of T cell activation-induced signals that lead to mitochondrial hyperpolarization. CD3/CD28 costimulation elicited 1) elevation of cytoplasmic and mitochondrial Ca^{2+} levels, 2) ROI production, 3) increased expression of endothelial NO synthase (eNOS) and neuronal NO synthase (nNOS) as well as NO production, and 4) mitochondrial hyperpolarization and subsequent mitochondrial swelling. Although Ca^{2+} release, ROI production, and NO production were diminished by IP_3R antagonist 2-aminoethoxydiphenyl borane (2-APB), superoxide dismutase mimic manganese (III) tetrakis (4-benzoic acid) porphyrin chloride (MnTBAP), spin trap 5-diisopropoxyphosphoryl-5-methyl-1-pyrroline-*N*-oxide (DIPPMPO), and NO chelator carboxy-2-phenyl-4,4,5,5-tetramethyl-imidazoline-1-oxyl-3-oxide (C-PTIO), mitochondrial hyperpolarization was only inhibited by C-PTIO and, to a lesser extent, by 2-APB. The results suggest that ROI- and Ca^{2+}-dependent NO production plays a dominant role in T cell activation-induced mitochondrial hyperpolarization.

Materials and Methods

Cell culture and T cell activation

PBMC were isolated from heparinized venous blood on Ficoll-Hypaque gradient. PBL were separated after the removal of monocytes by adherence to autologous serum-coated petri dishes (18). PBL were resuspended at 10^6 cells/ml in RPMI 1640 medium, supplemented with 10% FCS, 2 mM L-glutamine, 100 μg/ml penicillin, and 100 μg/ml gentamicin in 12-well plates at 37°C in a humidified atmosphere with 5% CO_2. For cross-linking of the CD3 Ag, tissue culture plates were precoated with 100 μg/ml goat anti-mouse IgG for 2 h at 37°C (ICN, Aurora, OH), washed once with PBS, and treated with 1 μg/ml OKT3 mAb per well (CRL 8001; American Type Culture Collection, Manassas, VA) for 1 h at 37°C before addition of 10^6 cells/ml PBL. CD28 costimulation was performed by addition of 500 ng/ml mAb CD28.2 (BD PharMingen, San Diego, CA).

Cell viability assays

Apoptosis was monitored by observing cell shrinkage and nuclear fragmentation, and quantified by flow cytometry after concurrent staining with FITC-conjugated annexin V (Annexin V^{FITC}; R&D Systems, Minneapolis, MN) (FL-1) and propidium iodide (PI) (FL-2) as earlier described (9). Staining with Cy5- or PE-conjugated annexin V (Annexin V^{PE}; R&D Systems) was used to monitor phosphatidyl serine (PS) externalization (FL-2) in parallel with measurement of ROI levels and $\Delta\psi_m$ (see below). Apoptosis rates were expressed as percentage of annexin V-positive/PI-negative cells. As earlier described (5, 9, 16, 19), live or apoptotic cells did not stain directly with PI and required permeabilization with 0.1% Triton X-100. When using hydroethidine (HE) (FL-2) for ROI measurement, cells were costained with Annexin V^{FITC} (R&D Systems) (FL-1). Thus, Annexin V^{PE} or Annexin V^{FITC} were matched with emission spectra of potentiometric and oxidation-, NO-, or Ca^{2+}-sensitive fluorescent probes. Specific combinations are described in each figure legend. Staining with annexin V alone or in combination with dihydrorhodamine 123 (DHR), HE, 5,6-carboxy-2′,7′-dichlorofluorescein (DCF), 3,3′-dihexyloxacarbocyanine iodide ($DiOC_6$), CMXRos, tetramethylrhodamine methyl ester (TMRM), 4-amino-5-methylamino-2′,7′-difluoroflourescein diacetate (DAF-FM), Fluo-3, or Rhod-2 (see next section below) was conducted in 10 mM HEPES (pH 7.4), 140 mM NaCl, and 2.5 mM $CaCl_2$.

Flow-cytometric analysis of ROI production and $\Delta\psi_m$

Production of ROI was assessed fluorometrically using oxidation-sensitive fluorescent probes 5,6-carboxy-2′,7′-dichlorofluorescein-diacetate, DHR, and HE (Molecular Probes, Eugene, OR) as earlier described (19). Following apoptosis assay, cells were washed three times in 5 mM HEPES-buffered saline (pH 7.4), incubated in HEPES-buffered saline with 0.1 μM DHR for 2 min, 1 μM 5,6-carboxy-2′,7′-dichlorofluorescein-diacetate for 15 min, or 1 μM HE for 15 min, and samples were analyzed using a BD Biosciences (Mountain View, CA) $FACStar^{Plus}$ flow cytometer equipped with tunable argon ion laser delivering 200 mW of power at 488 nm or LSRII flow cytometer equipped with 20-mW argon (emission at 488 nm) and 16-mW helium-neon lasers (emission at 634 nm). Fluorescence emission from DCF (green) or DHR (green) was detected at a wavelength of 530 ± 30 nm. Fluorescence emission from oxidized HE, ethidium (red), was detected at a wavelength of 605 nm. Dead cells and debris were excluded from the analysis by electronic gating of forward- and side-scatter measurements. Although R123, the fluorescent product of DHR oxidation, binds selectively to the inner mitochondrial membrane, ethidium and DCF remain in the cytosol of living cells. DHR and HE were more sensitive than DCF for measurement of ROI production. MnTBAP (300 μM), a superoxide dismutase mimic (20), and DIPPMPO (300 μM), a free-radical spin trap, reduced ROI levels and were used as inhibitors of ROI signaling, based on dose-response analyses.

$\Delta\psi_m$ was estimated by staining with 20 nM $DiOC_6$ (Molecular Probes), acationic lipophilic dye (21–23), for 15 min at 37°Cinthe dark before flow cytometry (excitation, 488 nm; emission, 525 nm; recorded in FL-1). Fluorescence of $DiOC_6$ is oxidation independent and correlates with $\Delta\psi_m$ (22). $\Delta\psi_m$ was also quantitated using a potential-dependent J-aggregate-forming lipophilic cation, 5,5 ‘,6,6′-tetrachloro-1,1 ‘,3,3 ‘-

tetraethylbenzimidazolocarbocyanine iodide (JC-1) (24). JC-1 selectively incorporates into mitochondria, where it forms monomers (fluorescence in green, 527 nm) or aggregates, at high transmembrane potentials (fluorescence in red, 590 nm) (24, 25). Cells were incubated with 0.5 μM JC-1 for 15 min at 37°C before flow cytometry. $\Delta\psi_m$ changes were also confirmed by staining with 1 μM CMXRos (excitation, 579 nm; emission, 599 nm; recorded in FL-2) and 1 μM TMRM (excitation, 543 nm; emission, 567 nm; recorded in FL-2; all from Molecular Probes). Cotreatment with a protonophore, 5 μM carbonyl cyanide m-chlorophenylhydrazone (Sigma-Aldrich, St. Louis, MO) for 15 min at 37°C resulted in decreased DHR, $DiOC_6$, CMXRos, TMRM, and JC-1 fluorescence and served as a positive control for disruption of $\Delta\psi_m$ (9). As altered incorporation of potentiometric dyes may represent a change in mitochondrial mass, the latter was monitored by staining with potential-insensitive mitochondrial dyes nonyl acridine orange (NAO; 50 nM; excitation, 490 nm; emission, 540 nm; recorded in FL-1; Molecular Probes) or MitoTracker Green-FM (100 nM; excitation, 490 nm; emission, 516 nm; recorded in FL-1; Molecular Probes). Using three-color fluorescence, mitochondrial ROI levels, $\Delta\psi_m$, and phosphatidyl serine externalization within T cell subsets were concurrently analyzed by parallel staining with DHR, DAF-FM, or $DiOC_6$ (FL-1), TMRM, Rhod-2, Annexin V^{PE} (FL-2), and PE-Cy5-conjugated mAb UCHT1 recognizing the CD3ε chain (Sigma-Aldrich), CD45RA, and CD45RO (BD PharMingen) (FL-3). Quantum Red contains two covalently linked fluorochromes, PE and Cy5. PE absorbs light energy at 488 nm and emits at 670 nm, in the excitation range of Cy5, which acts as an acceptor dye. Each measurement was conducted on 10,000 cells.

Measurement of intracellular NO levels

Production of NO was assessed by using DAF-FM (Molecular Probes) or a NO sensor kit (BD PharMingen). DAF-FM passively diffuses across cellular membranes; once inside cells, it is deacethylated by intracellular esterases and caged in the cell. DAF-FM is essentially nonfluorescent until it reacts with NO to form a fluorescent benzotriazole. Measurement of NO was calibrated by incubating PBL with NO donors (*Z*)-1-[2-(2-aminoethyl)-*N*-(2-ammonioethyl)amino]diazen-1-ium-1,2-diolate diethylenetriamine (NOC-18) (200 μM to 1.8 mM) or sodium nitroprusside (SNP) (400 μM to 10 mM). After testing 1–10 μM dye concentration during incubation times ranging from 10 min to 3 h, maximum NO sensitivity was achieved by loading cells with 1 μM DAF-FM for 2 h at 37°C. Excitation and emission maxima of DAF-FM are 495 and 515 nm, respectively. C-PTIO (500 μM), specific NO chelator (26), was used to reduce NO levels and inhibit NO signaling.

Measurement of cytoplasmic and mitochondrial calcium levels

Cytoplasmic calcium levels were measured by loading the cells with 1 μM fluoro-3 acetoxymethyl ester (Fluo-3/AM) (excitation, 506 nm; emission, 526 nm; recorded in FL-1; Molecular Probes). After entering the cell, AM hydrolysis occurs and the dye is caged in the cell. Fluoro-3 exhibit a large fluorescence intensity increase on binding calcium. Mitochondrial calcium level was estimated by loading the cells with 4 μM Rhod2/AM, which is compartmentalized into the mitochondria (27). 2-APB, a membrane-permeant antagonist of IP_3R, was used to inhibit T cell activation-induced Ca^{2+} signaling (28). Based

on testing a concentration range of 50 μM to 1 mM, 100 μM was found to achieve maximal inhibition of Ca^{2+} signaling.

Western blot analysis of NO synthase (NOS) expression

Control, CD3/CD28-, or H_2O_2-stimulated PBL were washed in PBS and resuspended in NOS solubilization buffer containing 10 mM HEPES (pH 7.4), 320 mM sucrose, 100 μM EDTA, 1.5 mM DTT, 10 μg/ml leupeptin, 10 μg/ml aprotinin, 1 mg/ml PMSF, and 10 μM tetrahydrobiopterin. After freezing and thawing thrice, the sample was pelleted by centrifugation in a microfuge at 15,000 × *g*, and the supernatant was used in subsequent experiments. Protein concentrations were determined by the Bradford method using the Bio-Rad (Hercules, CA) protein assay. Twenty micrograms of protein lysates were separated on a 7.5% SDS-polyacrylamide gel and electroblotted to nitrocellulose. Nitrocellulose strips were probed with NOS isoform-specific rabbit Abs. Ab to inducible NOS (iNOS) was directed to a C-terminal peptide (SLEMSAL), anti-nNOS was directed to residues 1411–1433, while eNOS Ab was raised against residues 599–613 (Calbiochem, San Diego, CA). As controls, blots were reprobed with β-actin-specific mouse Ab 1501R (Chemicon, Temecula, CA), as previously described (29). HRP-conjugated goat anti-rabbit IgG (Chemicon) was used as a secondary Ab for rabbit Abs, while biotin-conjugated goat anti-mouse IgG and streptavidin (Jackson ImmunoResearch Laboratories, West Grove, PA) were used as secondary and tertiary Abs, respectively, for detection of β-actin. Expression of NOS isoforms was visualized by ECL (Western Lightning Chemiluminescence Reagent Plus; PerkinElmer, Boston, MA), followed by detection of β-actin using 4-chloronaphthol. Automated densitometry was used to quantify the relative levels of protein expression using a Kodak Image Station 440CF with Kodak 1D Image Analysis software (Eastman Kodak, Rochester, NY).

ATP measurement

Intracellular ATP levels were determined using the luciferin-luciferase method (30). PBL (5×10^6) washed in PBS were resuspended in 50 μ1 of PBS with a 2.5% TCA. Such extracts were stored at −20°C. The total protein content of each sample was determined using the Lowry assay (31). The bioluminescence assay was performed in an AutoLumat LB953 automated luminometer (Berthold, Wildbad, Germany) using an ATP determination kit (Molecular Probes) according to the manufacturer's instructions. ATP standard curves were established in each experiment and were linear in the 5–15,000 nM range. To eliminate the impact of nonspecific inhibitors in the cellular extracts, standard amounts of ATP were added to the reaction mixtures as controls, and ATP levels were remeasured (32). The sample volume added to the reaction mixtures was <2% of the total assay volume.

Statistics

Results were analyzed by Student's *t* test or Mann-Whitney rank sum test for nonparametric data. Changes were considered significant at $p < 0.05$.

Results

CD3/CD28 costimulation elicits elevation of intracellular and mitochondrial Ca^{2+} levels, ROI and NO production, and mitochondrial hyperpolarization

Elevation of $\Delta\psi_m$ or mitochondrial hyperpolarization represents an early and reversible checkpoint associated with both T cell activation (5, 9) and apoptosis signals (9–15, 33). Previously, cross-linking of the TCR has been associated with elevation of cytosolic Ca^{2+} (34), and ROI (5, 8, 16) and NO production (35). In the present study, we investigated the contribution of these T cell activation signals to mitochondrial hyperpolarization. CD3/CD28 costimulation of human T lymphocytes increased cytoplasmic Ca^{2+} levels, by 25% after 20 min ($p = 0.03$), followed by further rises, 3.9 ± 0.75-fold after 4 h ($p < 0.001$) and 2.77 ± 0.75-fold after 24 h ($p = 0.0043$), respectively, as measured by Fluo-3 fluorescence (Fig. 1). In parallel, mitochondrial Ca^{2+} levels increased by 22% after 20 min ($p = 0.009$), 2.15 ± 0.5-fold after 4 h ($p < 0.001$), and 2.78 ± 0.8-fold after 24 h ($p = 0.001$), respectively, as measured by Rhod-2 fluorescence (Fig. 1). In comparison to baseline, cytoplasmic ROI levels increased to 1.32 ± 0.36-fold 20 min ($p = 0.026$), 1.53 ± 0.36-fold ($p = 0.002$) 4 h, and 4.57 ± 1.75-fold ($p < 0.001$) 24 h after T cell stimulation, as measured by HE fluorescence. Similar results were obtained using DCF, another oxidation-sensitive fluorescent probe (not shown). NO levels increased 6.09 ± 2.98-fold 4 h ($p < 0.001$) and 4.9 ± 1.8-fold 24 h after T cell stimulation ($p < 0.001$), as assessed by DAF-FM fluorescence (Fig. 1). Similar results were obtained with BD Bio-sciences NO sensor (not shown). Based on calibration with NO donors NOC-18 and SNP, full staining with the NO-sensitive fluorochromes required 2-h incubation at 37°C, thus preventing measurements at earlier time points. $\Delta\psi_m$ was elevated 1.73 ± 0.44-fold ($p < 0.001$) 4 h and 1.53 ± 0.17-fold ($p < 0.001$) 24 h after CD3/CD28 stimulation, as estimated by TMRM fluorescence. Similar $\Delta\psi_m$ elevations were obtained based on $DiOC_6$ fluorescence (Fig. 1). Although monocyte-depleted PBL were used for stimulation of CD3/CD28, we investigated whether NO was produced by T cells. Concurrent staining with PE-Cy5-conjugated mAb UCHT1 recognizing the TCR ε-chain showed that CD3/CD28 costimulation-induced elevation of cytosolic and mitochondrial Ca^{2+} levels, NO production, and mitochondrial hyperpolarization occurred within T lymphocytes (Fig. 2*A*). CD3/CD28 costimulation also resulted in appearance of a distinct population of T cells with elevated cytosolic and mitochondrial Ca^{2+} levels, NO production, and mitochondrial hyperpolarization (Fig. 2*A*). These changes similarly affected CD45RA and CD45RO cells (Fig. 2*B*).

IP_3R antagonist 2-APB and NO chelator C-PTIO inhibit CD3/CD28 costimulation-induced mitochondrial hyperpolarization

Mobilization of Ca^{2+} in response to TCR stimulation is dependent on generation of IP_3 and its binding to IP_3R present on intracellular calcium stores, such as endoplasmic reticulum (36). Release of Ca^{2+} into the cytosol subsequently activates Ca^{2+} influx through the plasma membrane (28). IP_3R-mediated Ca^{2+} signals are associated with large increases of mitochondrial matrix Ca^{2+} concentration (37). Ordering of T cell activation-induced signals —elevation of cytoplasmic and mitochondrial Ca^{2+} levels, ROI and NO production, and mitochondrial hyperpolarization—was investigated using selective inhibitors. CD3/CD28 costimulation-induced ROI production and, to a lesser extent, NO production and elevation

of cytoplasmic Ca^{2+} (Fig. 3*A*) were diminished by MnTBAP (300 μM), a superoxide dismutase mimic (Fig. 3, *B* and *F*). By contrast, MnTBAP failed to eliminate mitochondrial hyperpolarization (Fig. 3*F*). DIPPMPO (300 μM), a free-radical spin trap, had effects similar to MnTBAP (Fig. 3, *C* and *F*). The membrane-permeant IP_3R inhibitor 2-APB (100 μM) reduced elevation of cytoplasmic Ca^{2+}, NO production, and mitochondrial hyperpolarization 4 h after CD3/CD28 costimulation, as monitored by Fluo-3, DAF-FM, and TMRM fluorescence, respectively. 2-APB also diminished late ROI production (Fig. 3, *D* and *F*). C-PTIO (500 μM), specific NO chelator (26), reduced NO levels (−80 ± 7.5%; $p = 0.004$) and profoundly inhibited mitochondrial hyperpolarization (−85.0 ± 10.0%; $p = 0.008$), ROI production (−88 ± 19%; $p = 0.01$), and cytoplasmic (−75 ± 5.6%; $p < 0.001$) and mitochondrial Ca^{2+} elevation (−62 ± 10.0%; $p = 0.005$) as measured by DAF-FM, TMRM, HE, Fluo-3, and Rhod-2 fluorescence, respectively (Fig. 3, *E* and *F*). Due to its short half-life (26), C-PTIO affected signal intensities up to 4 h following CD3/CD28 costimulation. Mitochondrial swelling, as measured by NAO fluorescence, was reduced by C-PTIO ($p < 0.001$) at 4 hand by MnTBAP ($p = 0.01$) at 24 h following TCR stimulation, respectively.

NO induces coordinate elevation of cytosolic and mitochondrial Ca^{2+} levels, ROI production, and mitochondrial hyperpolarization

CD3/CD28 costimulation-induced mitochondrial hyperpolarization was inhibited by 2-APB and C-PTIO, suggesting involvement of Ca^{2+} influx and NO production. To assess a direct role of Ca^{2+} in mitochondrial hyperpolarization, PBL were exposed to calcium ATPase inhibitor thapsigargin (100 nM to 5 μM) and calcium ionophore ionomycin (100 nM to 5 μM), which deplete calcium stores independent of receptor-coupled events and promote calcium entry through the plasma membrane (28). Both ionomycin (2 μM) and thapsigargin (1 μM) markedly increased cytoplasmic and mitochondrial Ca^{2+} levels, as monitored by Fluo-3 and Rhod-2 fluorescence (Fig. 4, *A* and *D*). Neither ionomycin and nor thapsigargin affected $\Delta\psi_m$ or NO production. ROI production was increased 1.32 ± 0.16-fold ($p = 0.013$) by thapsigargin. Effect of NO on $\Delta\psi_m$ was evaluated by exposing PBL to NO donors NOC-18 (200 μM to 1.8 mM) or SNP (400 μM to 10 mM) (not shown). Treatment of human PBL with 600 μM NOC-18, capable of slowly releasing NO, increased DAF-FM fluorescence by 3.13 ± 0.8-fold after 4 h ($p = 0.04$) and 3.7 ± 0.6-fold after 24 h ($p = 0.03$). NOC-18 up to a concentration of 1.8 mM did not alter cell viability (data not shown). After 24 h of treatment of human PBL with NOC-18, $\Delta\psi_m$ was increased by 3.5 ± 0.79-fold ($p = 0.002$). NOC-18 also enhanced cytoplasmic and mitochondrial Ca^{2+} as well as ROI levels (Fig. 4, *C* and *D*). As expected (38), in comparison to control PBL (15.6 ± 0.8 $\Delta\psi_m$M), treatment with 600 μM NOC-18 for 24 h markedly reduced intracellular ATP concentrations (4.9 ± 0.3 μM; $p = 0.02$).

T cell activation resulted in the appearance of a cell population with elevated cytosolic and mitochondrial Ca^{2+} levels, ROI and NO production, and mitochondrial hyperpolarization detectable from 4 to 24 h following CD3/CD28 costimulation (Fig. 3*A*). Formation of such a cell population was abrogated by C-PTIO (Fig. 3*E*), whereas it was unaffected by 2-APB, DIPPMPO, and MnTBAP (Fig. 3, *B*–*D*). Similar to CD3/CD28 costimulation, treatment of PBL with NOC-18 led to the appearance of a distinct cell population with increased

cytosolic and mitochondrial Ca^{2+} levels, ROI and NO production, and mitochondrial hyperpolarization (Fig. 4, *C* and *D*). Raising Ca^{2+} levels by ionomycin and thapsigargin failed to elicit sustained mitochondrial hyperpolarization (Fig. 4, *A*, *B*, and *D*).

Interruption of T cell activation-induced Ca^{2+} signaling with the membrane-permeant IP_3R inhibitor 2-APB reduced elevation of cytoplasmic Ca^{2+}, and NO and ROI production. MnTBAP, a superoxide dismutase mimic (20), and DIPPMPO, free-radical spin trap (19), reduced ROI production and, to a lesser extent, NO production and elevation of cytoplasmic Ca^{2+}, whereas they failed to eliminate mitochondrial hyperpolarization or mitochondrial Ca^{2+} elevation. C-PTIO, specific NO chelator (26), exhibited the most profound inhibitory effect on T cell activation-induced NO productions (−80 ± 7.5%; $p = 0.004$), mitochondrial hyperpolarization (−85.0 ± 10.0%; $p = 0.008$), ROI production (−88 ± 19%; $p = 0.01$), and cytoplasmic (−75 ± 5.6%; $p < 0.001$) and mitochondrial Ca^{2+} elevation (−62 ± 10.0%; $p = 0.005$). Formation of a T cell population with elevated $\Delta\psi_m$ was completely abrogated by C-PTIO, but not by 2-APB, DIPPMPO, and MnTBAP (Fig. 4). Similar to CD3/CD28 costimulation, treatment of PBL with NOC-18 led to the appearance of a T cell subset with increased cytosolic and mitochondrial Ca^{2+} levels, ROI and NO production, and mitochondrial hyperpolarization, whereas raising intracellular Ca^{2+} by ionomycin or thapsigargin failed to elicit sustained mitochondrial hyperpolarization. Furthermore, inhibition of T cell activation-induced Ca^{2+} signaling by 2-APB was less effective than NO chelator C-PTIO in blocking $\Delta\psi_m$ elevation. Although ROI quenching by MnTBAP and DIPPMPO reduced ROI production and, to a lesser extent, NO production, they failed to influence $\Delta\psi_m$ elevation. These results suggested that T cell activation-induced ROI and Ca^{2+} signals contribute to NO production, with the latter representing a final and dominant step in mitochondrial hyperpolarization.

In accordance with previous studies (10), H_2O_2 elicited mitochondrial hyperpolarization, which was accompanied by elevation of cytoplasmic and mitochondrial Ca^{2+} and increased NO production. These changes were inhibited by MnTBAP, 2-APB, and C-PTIO (Fig. 5). The findings suggested that production of H_2O_2 and ROI may contribute to CD3/CD28-induced NO production and mitochondrial hyperpolarization.

Expression of eNOS and nNOS is enhanced by CD3/CD28 costimulation and H_2O_2 treatment

The following three isoforms of NOS have been delineated: 157-kDa nNOS, 140-kDa eNOS, and 135-kDa iNOS. As shown in Fig. 6, Western blot analysis of protein lysates from human PBL revealed expression of eNOS and nNOS and absence of iNOS, using isoform-specific Abs. With respect to β-actin, eNOS and nNOS protein levels were stimulated up to 15-fold by CD3/CD28 costimulation (Fig. 6*A*). Expression of eNOS and nNOS was also enhanced by treatment with 100 μM H_2O_2. Ionomycin or thapsigargin did not affect expression of eNOS and nNOS (not shown), in accordance with DAF-FM fluorescence measurements (Fig. 4*D*). Maximal stimulation of eNOS and nNOS expression was noted 24 h after CD3/CD28 costimulation and 4 h after treatment with H_2O_2, respectively, suggesting that T cell activation-induced NOS expression was delayed and depended on production of

H_2O_2 and ROI. Indeed, CD3/CD28 costimulation-induced NO production was inhibited by superoxide dismutase mimic MnTBAP and ROI spin trap DIPPMPO (Fig. 3*F*).

Discussion

Mitochondrial hyperpolarization or elevation of $\Delta\psi_m$ has emerged as a critical, early, and reversible checkpoint associated with both T cell activation (5, 9) and apoptosis (9–15, 33). T cell activation-induced mitochondrial hyperpolarization was associated with transient inhibition of F_0F_1-ATPase, ATP depletion, and sensitization to necrosis (16), suggesting that $\Delta\psi_m$ elevation is a critical checkpoint of T cell fate decisions. The present study demonstrates that mitochondrial hyperpolarization in T lymphocytes is associated with a dramatic increase, > 6-fold, of NO production lasting 4–24 h after CD3/CD28 costimulation. Investigation of molecular ordering of T cell activation-induced NO production revealed critical roles for ROI production and cytoplasmic and mitochondrial Ca^{2+} influx (Fig. 7). Accordingly, CD3/CD28 costimulation-induced ROI production or H_2O_2 enhanced expression of NOS isoforms eNOS and nNOS, which required elevated Ca^{2+} levels for enzymatic activity. These results suggested that T cell activation-induced ROI and Ca^{2+} signals contribute to NO production, with the latter representing a final and dominant step in mitochondrial hyperpolarization (Fig. 7). Indeed, NO has recently been recognized as a key signal mediating mitochondrial respiration (38) and biogenesis (39), thus supporting cellular activation and proliferation. NO also causes Ca^{2+} and ROI efflux from mitochondria (38), which are consistent with our findings. Concurrently, NO, acting as a competitive antagonist, can cause a reversible inhibition of cytochrome *c* oxidase complex IV, which may result in mitochondrial hyperpolarization (15) and ATP depletion (38). Intracellular ATP concentration is a key switch in the cell's decision to die via apoptosis or necrosis, and depletion of ATP predisposes for necrosis (5, 8).

NO is recognized as an important intercellular and intracellular messenger; however, its role in T cell activation has not been established. There are three known isoforms of NOS: nNOS, eNOS, and iNOS. Expression of eNOS has been previously demonstrated in human peripheral blood B and T lymphocytes (40, 41), whereas TCR activation was found to induce expression of nNOS by ZB4 murine T cell hybridoma cells (42). Western blot analysis revealed expression of eNOS and nNOS and absence of detectable iNOS in control and CD3/CD28-costimulated PBL. Unlike iNOS, eNOS and nNOS are inactive at baseline Ca^{2+} levels (43). Inhibition of T cell activation-induced NO production via interference of Ca^{2+} signaling by 2-APB is also consistent with involvement of eNOS or nNOS (38). Treatment with NO donor NOC-18 or CD3/CD28 costimulation resulted in similar patterns of transient ATP depletion, resulting in a transiently increased susceptibility to cell death via necrosis (16, 38). NO-induced ROI production may also facilitate necrosis via oxidation of cysteine residues in the active sites of caspases (8, 44).

ROI mediate signaling through the CD3/CD28 receptors. Endogenous H_2O_2 is generated by superoxide dismutase from ROIs, $O_2^{\hat{a}\acute{I}}$ or OH^-, in mitochondria (45). In turn, H_2O_2 is scavenged by catalase and glutathione peroxidase (46). Although H_2O_2 is freely diffusible, it has no unpaired electrons and, by itself, is not a ROI (45). Induction of apoptosis by H_2O_2 requires mitochondrial transformation into an ROI, e.g., OH^-, through the Fenton reaction

(45, 47). In accordance with previous studies (10), H_2O_2 elicited mitochondrial hyperpolarization, which was accompanied by elevation of cytoplasmic and mitochondrial Ca^{2+} and increased NO production. These findings were consistent with previous data on H_2O_2- and ROI-induced IP_3 production (48) and Ca^{2+} release from endoplasmic reticulum and mitochondrial Ca^{2+} stores (49–52). Treatment of PBL with NO donor NOC-18 alone also elicited ROI production and Ca^{2+} release, indicating a positive-feedback regulation between NO and ROI signaling (Fig. 7). Western blot analysis showed enhanced expression of eNOS and nNOS in CD3/CD28- or H_2O_2-stimulated PBL. This can be related to previous studies showing that both transcription rate and half-life of eNOS mRNA are enhanced by H_2O_2, 3.0- and 2.8-fold, respectively (53).

Activity of both eNOS and nNOS is turned on by elevation of Ca^{2+} and binding of Ca^{2+}/calmodulin. Expression of Ca-dependent NOS isoforms and absence of Ca-independent iNOS in PBL are consistent with involvement of CD3/CD28 costimulation-induced Ca^{2+} release in ensuing NO production. The present data are consistent with a key role for NO production in T cell activation-induced mitochondrial hyperpolarization, which, in turn, is regulated by Ca^{2+} and ROI at multiple levels

References

1. Lenardo M, Chan KM, Hornung F, McFarland H, Siegel R, Wang J, Zheng L. Mature T lymphocyte apoptosis—immune regulation in a dynamic and unpredictable antigenic environment. Annu. Rev. Immunol. 1999; 17:221. [PubMed: 10358758]
2. Koretzky GA, Boerth NJ. The role of adapter proteins in T cell activation. Cell. Mol. Life Sci. 1999; 56:1048. [PubMed: 11212321]
3. Gringhuis SI, Leow A, Voort EAPapendrecht-Van Der, Remans PH, Breedveld FC, Verweij CL. Displacement of linker for activation of T cells from the plasma membrane due to redox balance alterations results in hyporesponsiveness of synovial fluid T lymphocytes in rheumatoid arthritis. J. Immunol. 2000; 164:2170. [PubMed: 10657671]
4. Lewis RS. Calcium signaling mechanisms in T lymphocytes. Annu. Rev. Immunol. 2001; 19:497. [PubMed: 11244045]
5. Gergely P Jr, Niland B, Gonchoroff N, Pullmann R Jr, Phillips PE, Perl A. Persistent mitochondrial hyperpolarization, increased reactive oxygen intermediate production, and cytoplasmic alkalinization characterize altered IL-10 signaling in patients with systemic lupus erythematosus. J. Immunol. 2002; 169:1092. [PubMed: 12097418]
6. Hamilos DL, Wedner HJ. The role of glutathione in lymphocyte activation. I. Comparison of inhibitory effects of buthionine sulfoximine and 2-cyclohexene-1-one by nuclear size transformation. J. Immunol. 1985; 135:2740. [PubMed: 4031498]
7. Suthanthiran M, Anderson ME, Sharma VK, Meister A. Glutathione regulates activation-dependent DNA synthesis in highly purified normal human T lymphocytes stimulated via the CD2 and CD3 antigens. Proc. Natl. Acad. Sci. USA. 1990; 87:3343. [PubMed: 1970635]
8. Perl A, Gergely P Jr, Puskas F, Banki K. Metabolic switches of T-cell activation and apoptosis. Antioxid. Redox Signal. 2002; 4:427. [PubMed: 12215210]
9. Banki K, Hutter E, Gonchoroff N, Perl A. Elevation of mitochondrial transmembrane potential and reactive oxygen intermediate levels are early events and occur independently from activation of caspases in Fas signaling. J. Immunol. 1999; 162:1466. [PubMed: 9973403]
10. Puskas F, Gergely P, Banki K, Perl A. Stimulation of the pentose phosphate pathway and glutathione levels by dehydroascorbate, the oxidized form of vitamin C. FASEB J. 2000; 14:1352. [PubMed: 10877828]

11. Banki K, Hutter E, Gonchoroff NJ, Perl A. Molecular ordering in HIV-induced apoptosis: oxidative stress, activation of caspases, and cell survival are regulated by transaldolase. J. Biol. Chem. 1998; 273:11944. [PubMed: 9565623]
12. Li P-F, Dietz R, Harsdorf Rvon. p53 regulates mitochondrial membrane potential through reactive oxygen species and induces cytochrome *c*-independent apoptosis blocked by Bcl-2. EMBO J. 1999; 18:6027. [PubMed: 10545114]
13. Gottlieb E, Heiden MGVander, Thompson CB. Bcl-x_L prevents the initial decrease in mitochondrial membrane potential and subsequent reactive oxygen species production during tumor necrosis factor α-induced apoptosis. Mol. Cell. Biol. 2000; 20:5680. [PubMed: 10891504]
14. Scarlett JL, Sheard PW, Hughes G, Ledgerwood EC, Ku H-H, Murphy MP. Changes in mitochondrial membrane potential during staurosporin-induced apoptosis in Jurkat cells. FEBS Lett. 2000; 475:267. [PubMed: 10869569]
15. Almeida A, Almeida J, Bolanos JP, Moncada S. Different responses of astrocytes and neurons to nitric oxide: the role of glycolytically generated ATP in astrocyte protection. Proc. Natl. Acad Sci. USA. 2001; 98:15294. [PubMed: 11742096]
16. Gergely P Jr, Grossman C, Niland B, Puskas F, Neupane H, Allam F, Banki K, Phillips PE, Perl A. Mitochondrial hyperpolarization and ATP depletion in patients with systemic lupus erythematosus. Arthritis Rheum. 2002; 46:175. [PubMed: 11817589]
17. Stryer, L. Biochemistry. New York: Freeman; p. 397
18. Perl A, Gonzalez-Cabello R, Lang I, Gergely P. Effector activity of $OKT4^+$ and $OKT8^+$ T-cell subsets in lectin-dependent cell-mediated cytotoxicity against adherent HEp-2 cells. Cell. Immunol. 1984; 84:185. [PubMed: 6230158]
19. Banki K, Hutter E, Colombo E, Gonchoroff NJ, Perl A. Glutathione levels and sensitivity to apoptosis are regulated by changes in transaldolase expression. J. Biol. Chem. 1996; 271:32994. [PubMed: 8955144]
20. Day BJ, Shawen S, Liochev SI, Crapo JD. A metalloporphyrin superoxide dismutase mimetic protects against paraquat-induced endothelial cell injury, in vitro. J. Pharmacol. Exp. Ther. 1995; 275:1227. [PubMed: 8531085]
21. Petit PX, O'Connor JE, Grunwald D, Brown SC. Analysis of the membrane potential of rat- and mouse-liver mitochondria by flow cytometry and possible applications. Eur. J. Biochem. 1990; 194:389. [PubMed: 2269275]
22. Tanner MK, Wellhausen SR, Klein JB. Flow cytometric analysis of altered mononuclear cell transmembrane potential induced by cyclosporin. Cytometry. 1993; 14:59. [PubMed: 8432204]
23. Xiang J, Chao DT, Korsmeyer SJ. BAX-induced cell death may not require interleukin β-converting enzyme-like proteases. Proc. Natl. Acad. Sci. USA. 1996; 93:14559. [PubMed: 8962091]
24. Smiley ST, Reers M, Mottola-Hartshorn C, Lin M, Chen A, Smith TW Jr, Steele GD, Chen LBo. Intracellular heterogeneity in mitochondrial membrane potentials revealed by a J-aggregate-forming cation JC-1. Proc. Natl. Acad. Sci. USA. 1991; 88:3671. [PubMed: 2023917]
25. Cossarizza A, Franceschi C, Monti D, Salvioli S, Bellesia E, Rivabene R, Biondo L, Rainaldi G, Tinari A, Malorni W. Protective effect of *N*-acetylcysteine in tumor necrosis factor-a-induced apoptosis in U937 cells: the role of mitochondria. Exp. Eye Res. 1995; 220:232.
26. Akaike T, Yoshida M, Miyamoto Y, Sato K, Kohno M, Sasamoto K, Miyazaki K, Ueda S, Maeda H. Antagonistic action of imidazolineoxyl *N*-oxides against endothelium-derived relaxing factor/.NO through a radical reaction. Biochemistry. 1993; 32:827. [PubMed: 8422387]
27. Hajnoczky G, Robb-Gaspers LD, Seitz MB, Thomas AP. Decoding of cytosolic calcium oscillations in the mitochondria. Cell. 1995; 82:415. [PubMed: 7634331]
28. Broad LM, Braun FJ, Lievremont JP, Bird GS, Kurosaki T, Putney JW Jr. Role of the phospholipase C-inositol 1,4,5-trisphosphate pathway in calcium release-activated calcium current and capacitative calcium entry. J. Biol. Chem. 2001; 276:15945. [PubMed: 11278938]
29. Banki K, Halladay D, Perl A. Cloning and expression of the human gene for transaldolase: a novel highly repetitive element constitutes an integral part of the coding sequence. J. Biol. Chem. 1994; 269:2847. [PubMed: 8300619]

30. Lundin A. Use of firefly luciferase in ATP-related assays of biomass, enzymes, and metabolites. Methods Enzymol. 2000; 305:346. [PubMed: 10812612]
31. Lowry OH, Rosebrough NJ, Farr AL, Randall RJ. Protein measurement with the Folin phenol reagent. J. Biol. Chem. 1951; 193:265. [PubMed: 14907713]
32. Lundin, A. ATP extractants neutralized by cyclodextrins. In: Campbell, AK.; Kricka, LJ.; Stanley, PE., editors. Biolumimescence and Chemiluminescence. Wiley: Chichester; 1994. p. 399
33. Sanchez-Alcazar JA, Ault JG, Khodjakov A, Schneider E. Increased mitochondrial cytochrome *c* levels and mitochondrial hyperpolarization precede camptothecin-induced apoptosis in Jurkat cells. Cell Death Differ. 2000; 7:1090. [PubMed: 11139283]
34. Stridh H, Gigliotti D, Orrenius S, Cotgreave I. The role of calcium in pre- and postmitochondrial events in tributyltin-induced T-cell apoptosis. Biochem. Biophys. Res. Commun. 1999; 266:460. [PubMed: 10600525]
35. Tai XG, Toyo-oka K, Yamamoto N, Yashiro Y, Mu J, Hamaoka T, Fujiwara H. Expression of an inducible type of nitric oxide (NO) synthase in the thymus and involvement of NO in deletion of TCR-stimulated double-positive thymocytes. J. Immunol. 1997; 158:4696. [PubMed: 9144482]
36. da Silva CP, Guse AH. Intracellular Ca^{2+} release mechanisms: multiple pathways having multiple functions within the same cell type? Biochim. Biophys. Acta. 2000; 1498:122. [PubMed: 11108956]
37. Pozzan T, Magalhaes P, Rizzuto R. The comeback of mitochondria to calcium signalling. Cell Calcium. 2000; 28:279. [PubMed: 11115367]
38. Brown GC. Nitric oxide and mitochondrial respiration. Biochim. Biophys. Acta. 1999; 1411:351. [PubMed: 10320668]
39. Nisoli E, Clementi E, Paolucci C, Cozzi V, Tonello C, Sciorati C, Bracale R, Valerio A, Francolini M, Moncada S, Carruba MO. Mitochondrial biogenesis in mammals: the role of endogenous nitric oxide. Science. 2003; 299:896. [PubMed: 12574632]
40. Reiling N, Kroncke R, Ulmer AJ, Gerdes J, Flad HD, Hauschildt S. Nitric oxide synthase: expression of the endothelial, Ca^{2+}/calmodulin-dependent isoform in human B and T lymphocytes. Eur. J. Immunol. 1996; 26:511. [PubMed: 8605914]
41. Sciorati C, Rovere P, Ferrarini M, Heltai S, Manfredi AA, Clementi E. Autocrine nitric oxide modulates CD95-induced apoptosis in γ/ä T lymphocytes. J. Biol. Chem. 1997; 272:23211. [PubMed: 9287328]
42. Williams MS, Noguchi S, Henkart PA, Osawa Y. Nitric oxide synthase plays a signaling role in TCR-triggered apoptotic death. J. Immunol. 1998; 161:6526. [PubMed: 9862677]
43. Bogdan C. Nitric oxide and the immune response. Nat. Immunol. 2001; 2:907. [PubMed: 11577346]
44. Sen CK, Sashwati R, Packer L. Fas mediated apoptosis of human Jurkat T-cells: intracellular events and potentiation by redox-active α-lipoic acid. Cell Death Differ. 1999; 6:481. [PubMed: 10381641]
45. Halliwell B, Gutteridge JM. Role of free radicals and catalytic metal ions in human disease: an overview. Methods Enzymol. 1990; 186:1. [PubMed: 2172697]
46. Mayes, PA. The pentose phosphate pathway and other pathways of hexose metabolism. In: Murray, RK.; Granner, DK.; Mayes, PA.; Rodwell, VW., editors. Harper's Biochemistry. Norwalk, CT: Appleton & Lange; 1993. p. 201
47. Skulachev VP. Mitochondrial physiology and pathology; concepts of programmed death of organelles, cells and organisms. Mol. Aspects Med. 1999; 20:139. [PubMed: 10626278]
48. Golub MS, Zhang W, Keen CL, Goldkorn T. Cellular actions of Al at low (1.25 microM) concentrations in primary oligodendrocyte culture. Brain Res. 2002; 941:82. [PubMed: 12031550]
49. Bielefeldt K, Whiteis CA, Sharma RV, Abboud FM, Conklin JL. Reactive oxygen species and calcium homeostasis in cultured human intestinal smooth muscle cells. Am. J. Physiol. 272:G1439. [PubMed: 9227480]
50. Suzuki YJ, Ford GD. Redox regulation of signal transduction in cardiac and smooth muscle. J. Mol. Cell. Cardiol. 1999; 31:345. [PubMed: 10093047]

51. Pariente JA, Camello C, Camello PJ, Salido GM. Release of calcium from mitochondrial and nonmitochondrial intracellular stores in mouse pancreatic acinar cells by hydrogen peroxide. J. Membr. Biol. 2001; 179:27. [PubMed: 11155207]

52. Hu Q, Yu ZX, Ferrans VJ, Takeda K, Irani K, Ziegelstein RC. Critical role of NADPH oxidase-derived reactive oxygen species in generating Ca^{2+} oscillations in human aortic endothelial cells stimulated by histamine. J. Biol. Chem. 2002; 277:32546. [PubMed: 12093794]

53. Drummond GR, Cai H, Davis ME, Ramasamy S, Harrison DG. Transcriptional and posttranscriptional regulation of endothelial nitric oxide synthase expression by hydrogen peroxide. Circ. Res. 2000; 86:347. [PubMed: 10679488]

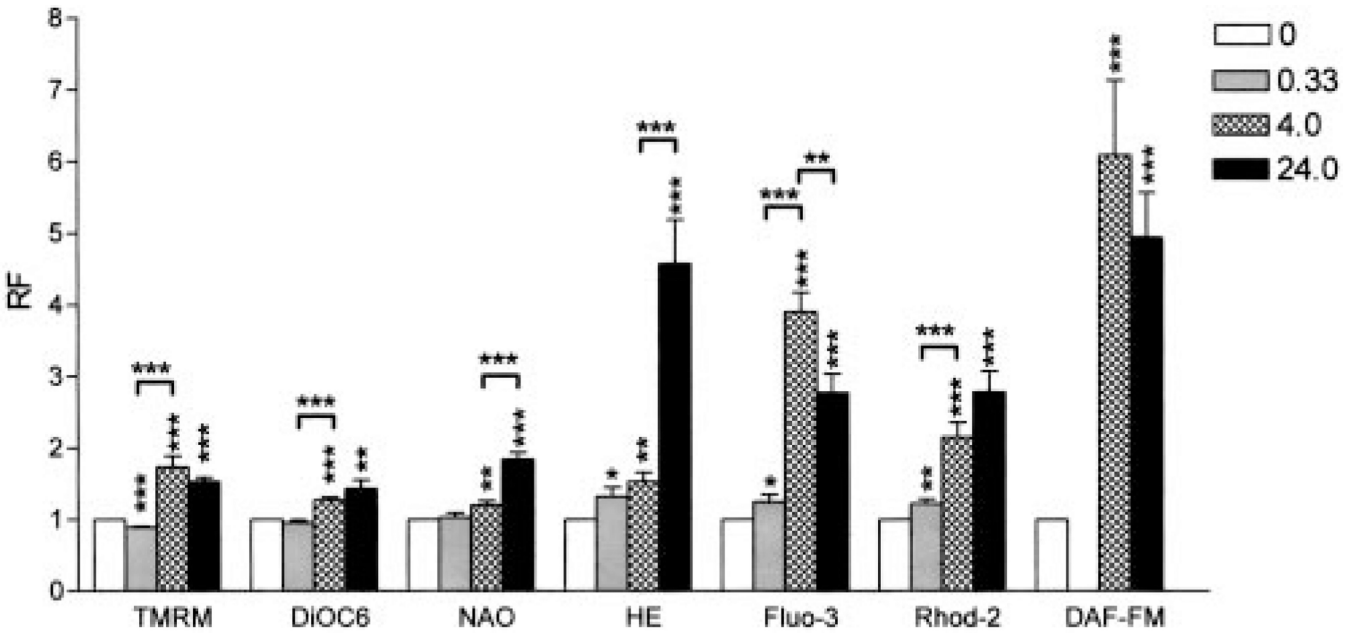

FIGURE 1.

Effect of CD3/CD28 costimulation on the $\Delta\psi_m$, mitochondrial mass, ROI levels, cytoplasmic and mitochondrial Ca^{2+} levels, and NO production. Normal human PBL were treated with CD3/CD28 Abs and assayed after incubation at 37°C for 20 min (0.33 h), 4 h, and 24 h $\Delta\psi_m$ was monitored by TMRM and $DiOC_6$; mitochondrial mass was measured by NAO; ROI production was assessed by HE; cytoplasmic and mitochondrial Ca^{2+} levels were assessed by Fluo-3 and Rhod-2; and NO production was monitored by DAF-FM fluorescence. Results were expressed as relative fluorescence (RF) values with respect to those of unstimulated cells normalized at 1.0. Data present mean ± SE of eight independent experiments. Values of *p* (*, <0.05; **, <0.01; ***, <0.001) above each column reflect comparison to untreated cells, whereas *p* values over brackets represent differences between the time points indicated.

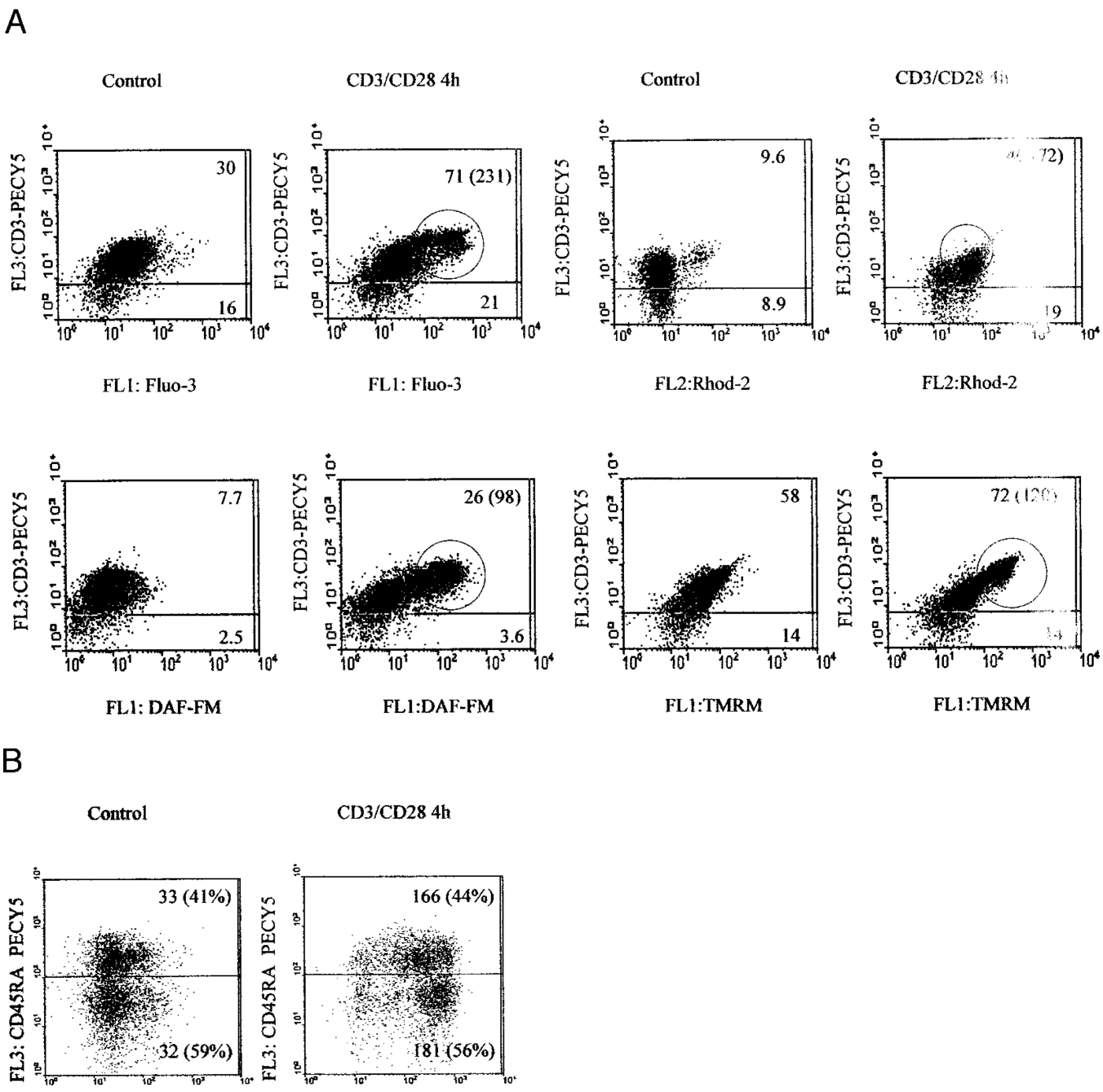

FIGURE 2.

A, Mitochondrial hyperpolarization is associated with increased NO production in T cells. Following CD3/CD28 costimulation, $\Delta\psi_m$ was measured by TMRM fluorescence (FL-2), cytoplasmic and mitochondrial Ca^{2+} levels were assessed by Fluo-3 (FL-1) and Rhod-2 fluorescence (FL-2), whereas NO production was monitored by DAF-FM fluorescence (FL-1). T cells were detected by staining with PE-Cy5-conjugated anti-CD3ε mAb UCHT1 (FL-3). Values in dot plots indicate mean channel fluorescence of $CD3^+$ and $CD3^-$ cells, respectively. Values in parentheses correspond to encircled high-mean channel fluorescence population within the $CD3^+$ T cell compartment, observed upon CD3/CD28 costimulation;

B, Following CD3/CD28 costimulation, NO production was monitored by DAF-FM fluorescence (FL-1), and CD45RA T cells were detected by staining with PE-Cy5-conjugated anti-CD45RA mAb (FL-3).

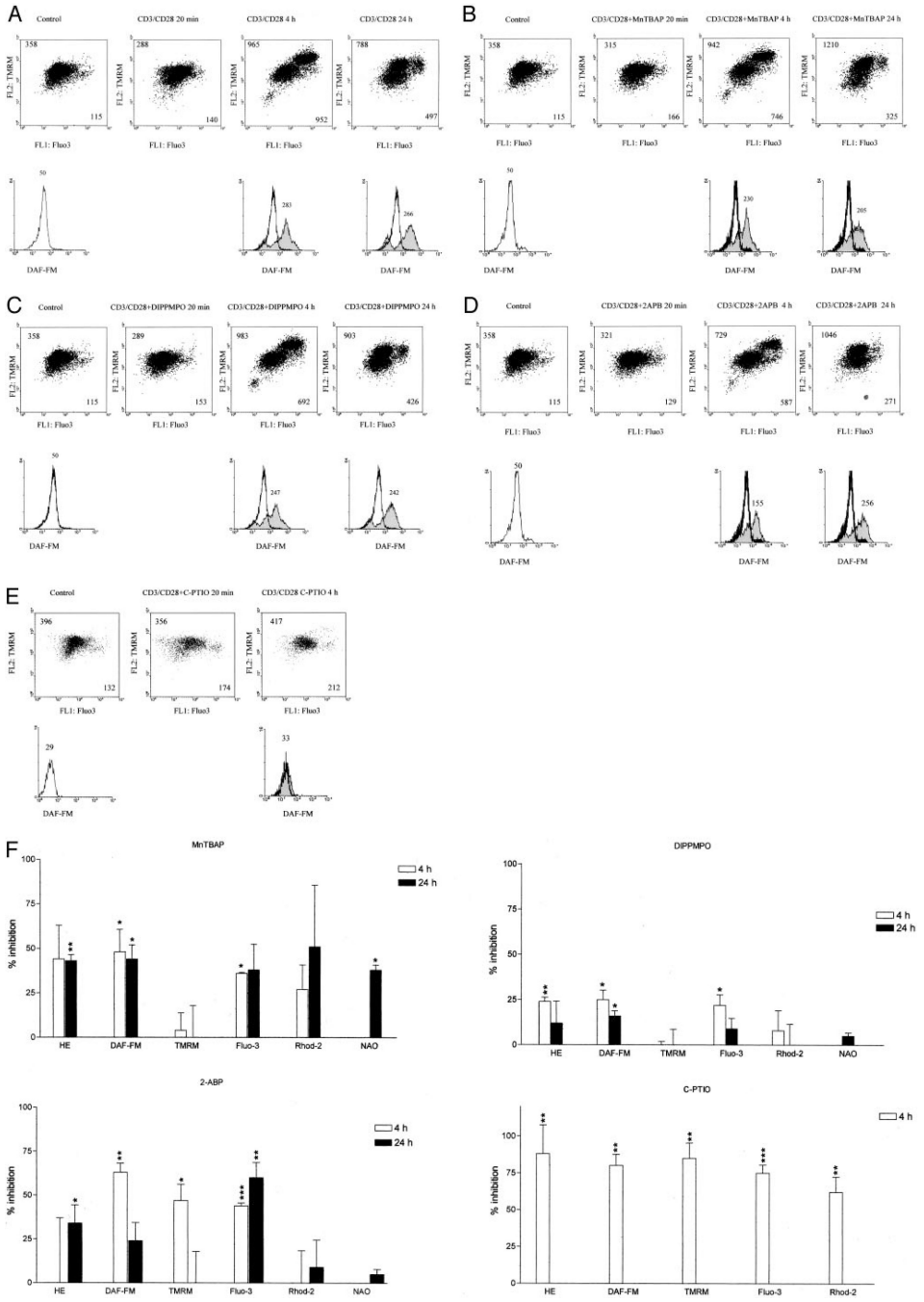

FIGURE 3.

Effect of MnTBAP, DIPPMPO, 2-APB, and C-PTIO on T cell activation-induced mitochondrial hyperpolarization, cytoplasmic and mitochondrial Ca^{2+} levels, and ROI and NO production. Values in dot plots (*row 1*) indicate mean channel FL-1 and FL-2 fluorescence, respectively. Values over histograms (*row 2*) indicate mean channel of DAF-FM fluorescence (FL-1). Histograms of CD3/CD28 costimulated cells (shaded curves) are overlaid on control cells (open curves); *A*, CD3/CD28 costimulation leads to mitochondrial hyperpolarization with appearance of a cell population with elevated $\Delta\psi_m$, Ca^{2+} levels, and

NO production; *B*, Effect of MnTBAP on CD3/CD28-induced elevation of $\Delta\psi_m$ Ca^{2+} levels, and NO production; *C*, Effect of DIPPMPO on CD3/CD28-induced elevation of $\Delta\psi_m$, Ca^{2+} levels, and NO production; *D*, Effect of 2-APB on CD3/CD28-induced elevation of $\Delta\psi_m$ Ca^{2+} levels, and NO production; *E*, Effect of C-PTIO on CD3/CD28-induced elevation of $\Delta\psi_m$ Ca^{2+} levels, and NO production; *F*, Percentage of inhibition of T cell activation-induced changes in $\Delta\psi_m$, mitochondrial mass, ROI levels, cytoplasmic and mitochondrial Ca^{2+} levels, and NO production monitored by TMRM, NAO, HE, Fluo-3, Rhod-2, and DAF-FM fluorescence, respectively. Data represent mean ± SE of four independent experiments. Values of *p* (*, <0.05; **, <0.01; ***, <0.001) above each column reflect comparison to untreated cells.

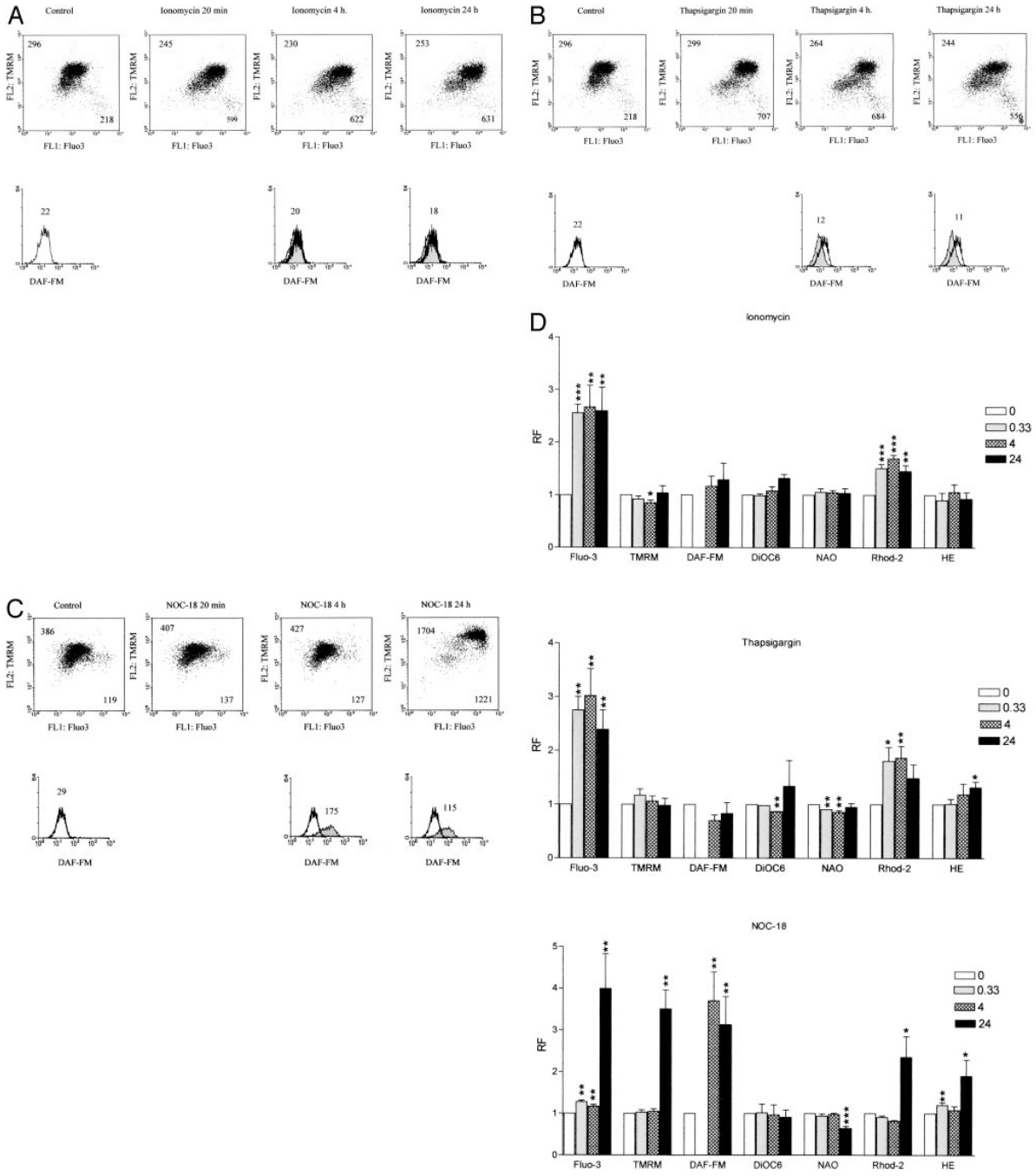

FIGURE 4.

Effect of ionomycin (*A*), thapsigargin (*B*), and NOC-18 (*C*) on $\Delta\psi_m$, Ca^{2+} levels, and NO production. Values in dot plots (*row 1*) indicate mean channel FL-1 and FL-2 fluorescence, respectively. Values over histograms (*row 2*) indicate mean channel of DAF-FM fluorescence (FL-1). Histograms of treated cells (shaded curves) are overlaid on control cells (open curves); *D*, Shown are ionomycin-, thapsigargin-, and NOC-18-induced changes in $\Delta\psi_m$, mitochondrial mass, ROI levels, cytoplasmic and mitochondrial Ca^{2+} levels, and NO production monitored by TMRM, NAO, HE, Fluo-3, Rhod-2, and DAF-FM fluorescence,

respectively. Data represent mean ± SE of four independent experiments. Values of *p* (*, <0.05; **, <0.01; ***, <0.001) above each column reflect comparison to untreated cells.

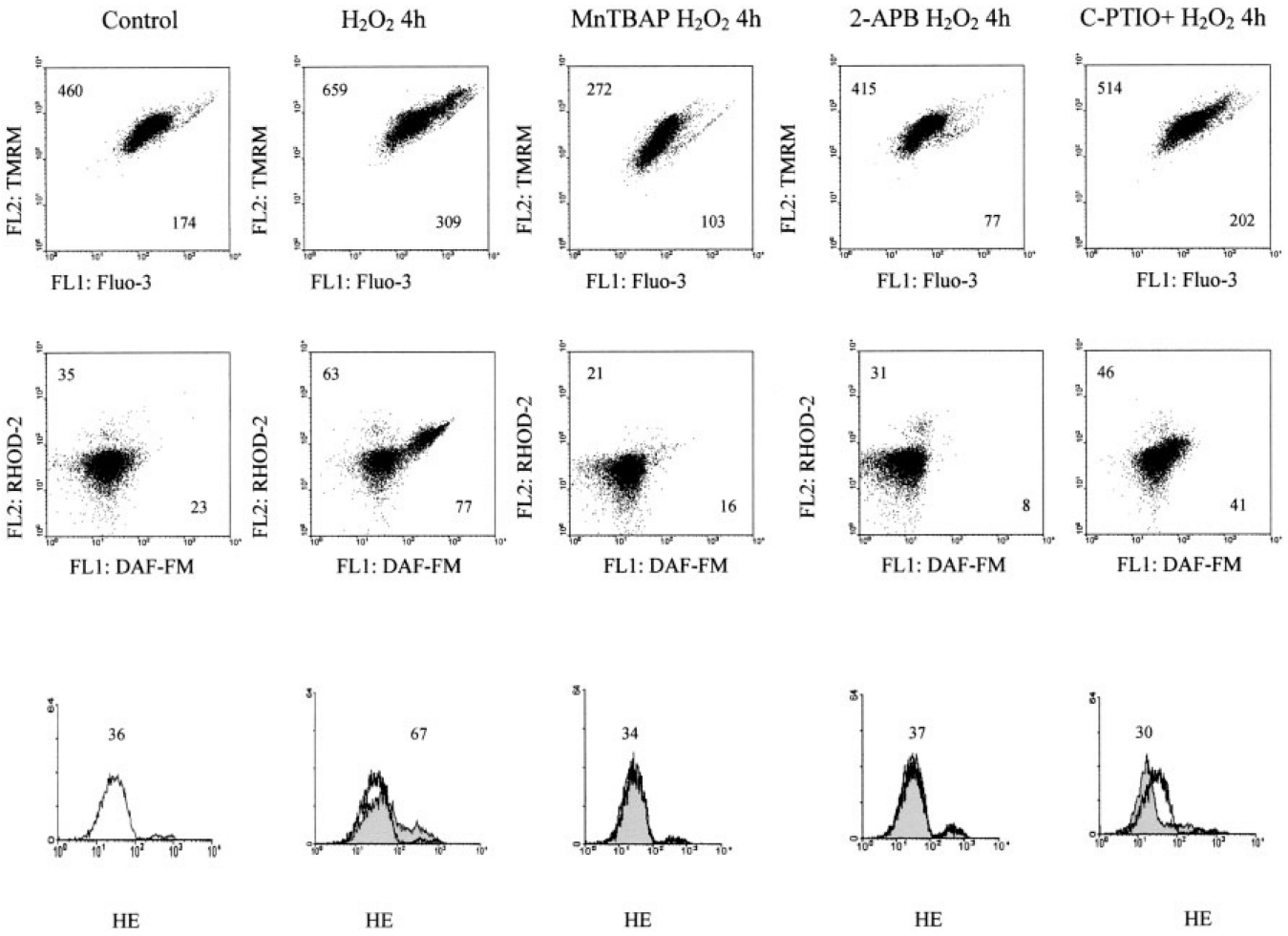

FIGURE 5.

Effect of MnTBAP, 2-APB, and C-PTIO on H_2O_2-induced mitochondrial hyperpolarization, cytoplasmic and mitochondrial Ca^{2+} levels, and NO and ROI production as monitored by TMRM, Fluo-3, Rhod-2, DAF-FM, and HE fluorescence, respectively. Live-cell staining with annexin V-Cy5 (FL-3) (not shown) were analyzed. Values in dot plots reflect mean channel FL-1 and FL-2 fluorescence (*rows 1* and *2*). Values over histograms (*row 3*) indicate mean channel of HE fluorescence (FL-2). Histograms of H_2O_2-treated cells (shaded curves) are overlaid on untreated cells (open curves).

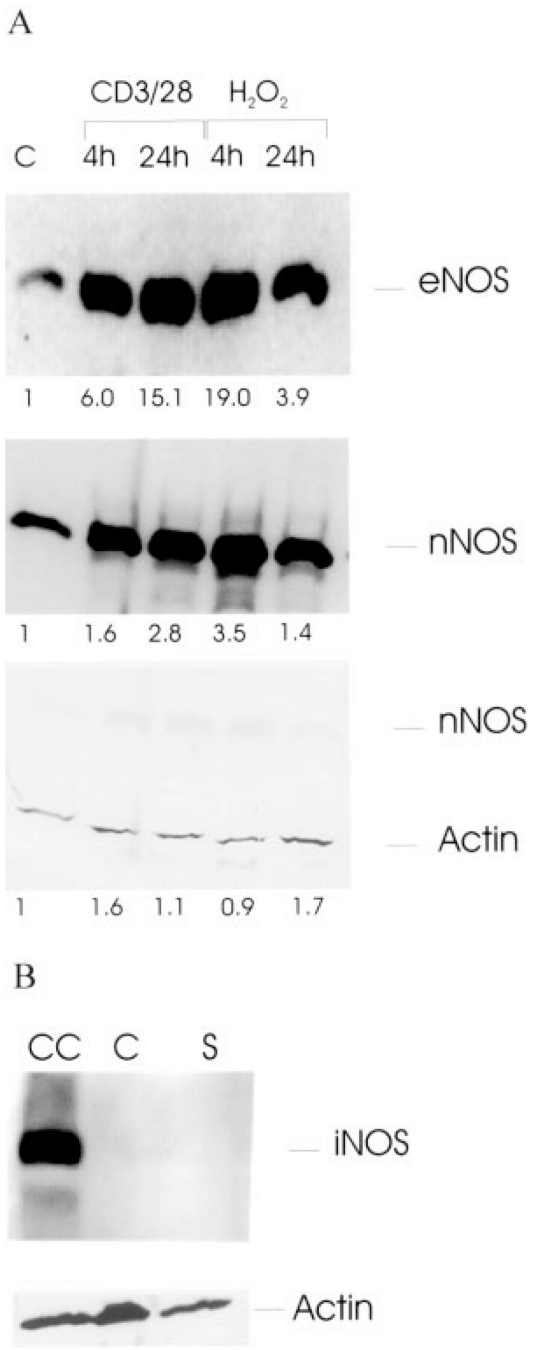

FIGURE 6.

A, Western blot analysis of eNOS and nNOS expression in response to CD3/CD28 costimulation or treatment with 100 μM H_2O_2. Twenty micrograms of protein lysates were loaded in each lane, separated in a 7.5% SDS-PAGE gel, transferred to nitrocellulose, and probed with Abs specific for NOS isoforms eNOS and nNOS. Subsequently, blots were reprobed with control Ab to human β-actin. Values below lanes indicate relative expression of NOS isoforms in CD3/CD28- or H_2O_2-treated vs control PBL (C) calculated by automated densitometry using β-actin levels as baseline; *B*, Western blot analysis of iNOS

expression in control (C) and CD3/CD28 costimulated PBL (S). CC, Chondrocyte protein lysate used as positive control for iNOS expression. Subsequently, the blot was reprobed with control Ab to human β-actin.

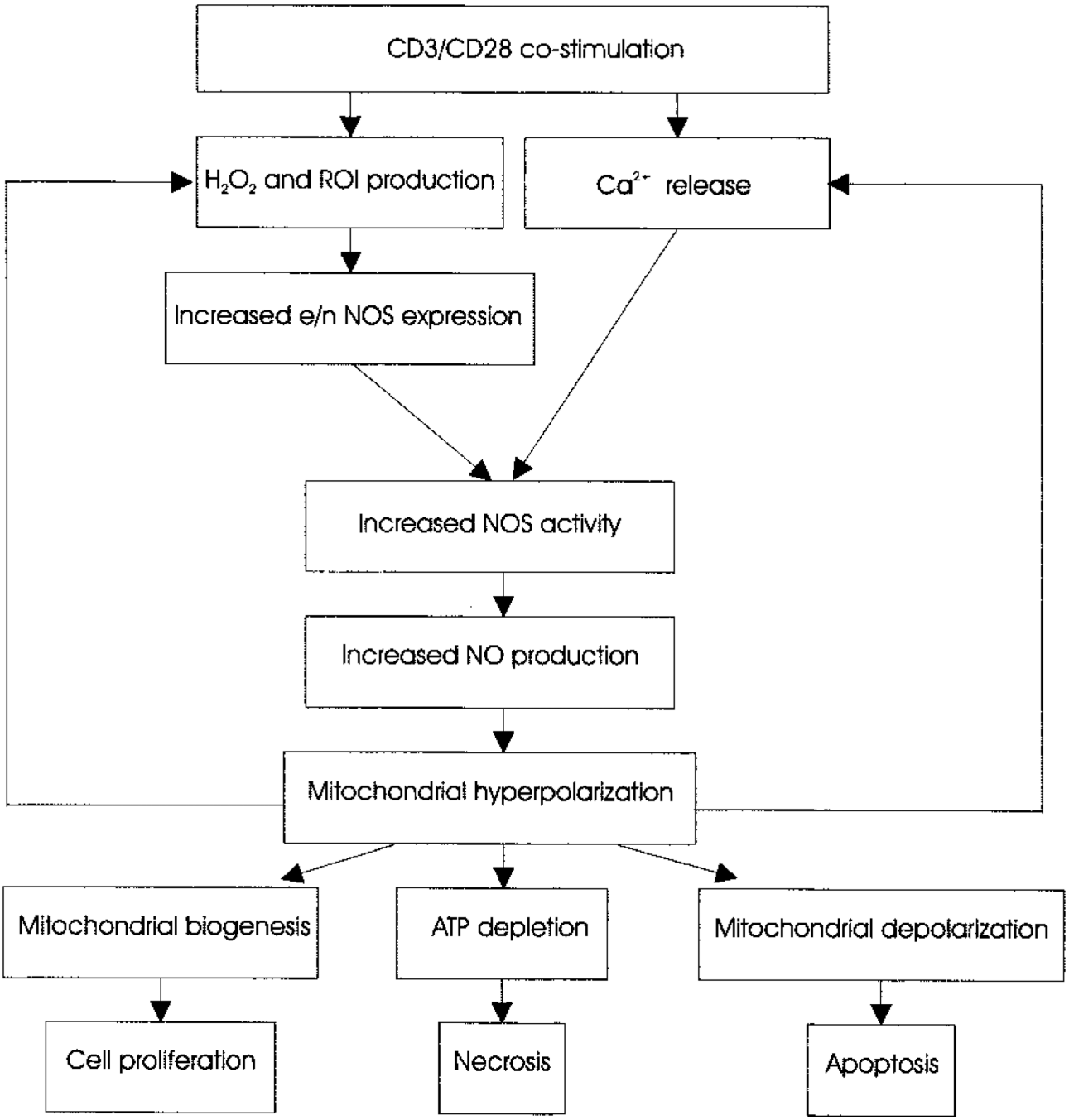

FIGURE 7.
Schematic ordering of CD3/CD28 costimulation-induced mitochondrial signals in human T lymphocytes.